4th Flow Control Conference
Seattle, WA June 23 - 26, 2008

AIAA-2008-4195
SAND2008-3711C

A Snapshot Decomposition Method for Reduced Order Modeling and Boundary Feedback Control

R. C. Camphouse [1]
Sandia National Laboratories
Performance Assessment and Decision Analysis Department

J. H. Myatt and R. F. Schmit
Air Force Research Laboratory
Air Vehicles Directorate

M. N. Glauser, J. M. Ausseur, M. Y. Andino, and R. D. Wallace
Syracuse University
Department of Mechanical Engineering

Abstract

In this paper, we develop a reduced basis construction method that allows for separate consideration of baseline and actuated dynamics in the reduced modeling process. A prototype initial boundary value problem, governed by the two-dimensional Burgers equation, is formulated to demonstrate the utility of the method in a boundary control setting. Comparisons are done between reduced and full order solutions under open-loop boundary actuation to illustrate advantages gained by separate consideration of actuated dynamics. A tracking control problem is specified using a linear quadratic regulator formulation. Comparisons of feedback control effectiveness are done to demonstrate benefits in control effectiveness obtained from separate consideration of actuated dynamics during model reduction.

Nomenclature

L	covariance matrix
S	solution snapshot
N	total number of snapshots
T	actuated snapshot
N_A	total number of actuated snapshots
ϕ, α	basis mode and temporal coefficient, respectively
M	number of basis modes
M_B, M_A	number of baseline and actuator modes, respectively
ξ, η	baseline and actuator mode, respectively
θ, β	baseline and actuator mode temporal coefficient, respectively
λ, v	eigenvalue and eigenvector, respectively
A, B	state and control matrices, respectively
G, F	nonlinear and forcing matrices, respectively
Q, R	state and control weight matrices, respectively
γ	control robustness parameter
Ω	spatial domain
t	time
$\mathbf{x}$	spatial coordinate vector
h	spatial step-size

Introduction

Reduced order modeling has received significant research attention in recent years. For many problems of practical interest, the order of the system describing the application must be reduced. An illustrative example where this is required is the development of feedback control laws for fluid flow configurations. It is not uncommon for discretized flow models to describe millions of state variables.[1] Unfortunately, the development of systematic feedback control laws from systems of such large dimension is a computationally intractable problem. For example, if one uses a linear quadratic regulator (LQR) control formulation, roughly 10^{12} Riccati unknowns need to be calculated for a discretized flow model describing 10^6 states. The Riccati

unknowns are solutions to a nonlinear matrix equation.[2] Existing computing power and computational algorithms are not capable of solving an LQR problem of such large dimension. For dynamical models that are very large scale, such as those describing fluid flow configurations, it is apparent that the order of the system must be reduced prior to control law design.[3]

Several research efforts have been concerned with, or relied upon, the development of order reduction strategies that provide reduced order models in a form amenable to state-space feedback control law design.[4–14] For the case of boundary control, the development of such models has been an open problem. For many applications of practical interest, such as feedback control of the air flow over an airplane wing, boundary actuation is a requirement. These applications require actuation to be located on the surface if they are to be implemented in hardware in the physical system. Most reduced modeling efforts have either been concerned with the case of control action via a body force or have approximated boundary actuation by a body force on the domain interior. Few techniques have been obtained thus far providing reduced order models with explicit boundary input that can be used for systematic design of feedback control laws. It is difficult to extract the boundary control input in the reduced model. When proper orthogonal decomposition (POD) is used in conjunction with Galerkin projection, boundary conditions are absorbed in the process. An additional step is required to make the action of the control input explicit in the model.

Recent inroads have allowed for accurate implementation of boundary control in reduced order state-space models. One approach is to capture the influence of boundary actuation indirectly. Of note is the work of Serrani and Kasnakoğlu[15] where a basis representing the influence of boundary actuation is captured by solving a particular optimization problem in L^2. The dimensions of reduced order dynamical models constructed with this method are typically very small, allowing for implementation of nonlinear control techniques where small system order is critical. Other methods utilize POD in combination with a weak formulation of the Galerkin projection.[16–19] The advantage of a weak formulation is that boundary conditions appear naturally when the reduced model is written weakly. Posing the system weakly also reduces regularity requirements of the solution, reducing errors that result from numerical approximation of high order derivatives in the Galerkin system. In this paper, we utilize a method[16] incorporating difference approximations in the weak formulation to construct reduced models with boundary control input appearing explicitly.

Finally, order reduction methods must be flexible so that they are amenable to either simulation or experimental approaches. Each approach has advantages and disadvantages, but the particular application at hand often dictates the approach taken. Methods solely suitable for a simulation approach will not likely lend themselves to implementation in an experimental facility. There is currently a need for order reduction strategies, suitable for practical control configurations, that can utilize system data generated by simulation or experiment. It is in this spirit that the techniques presented in this paper are developed. Simulation data is used to demonstrate methods in the current paper. The application of these methods to an experimental laser turret configuration is presented in a companion paper.[20]

Proper Orthogonal Decomposition

Proper orthogonal decomposition is a popular technique used to construct optimal basis functions attractive for reduced order modeling. In this work, we use a POD algorithm[21] based on the snapshot method[22] to construct the low order basis needed for the development of the reduced order model. For the sake of completeness and clarity in what follows, we briefly describe this technique. A data ensemble of snapshots $\{S_i(\mathbf{x})\}_{i=1}^N$ is generated for the system via numerical simulation or experiment, where N is the total number of snapshots. Each snapshot consists of instantaneous system data. With the snapshot ensemble in hand, the $N \times N$ correlation matrix L defined by

$$L_{i,j} = \langle S_i, S_j \rangle \tag{1}$$

is constructed. In this work, we utilize the standard $L^2(\Omega)$ inner product

$$\langle S_i, S_j \rangle = \int_\Omega S_i S_j^* \mathbf{dx}, \tag{2}$$

where S_j^* denotes the complex conjugate of S_j, in the construction of L.

The eigenvalues $\{\lambda_i\}_{i=1}^N$ of L are calculated and sorted in descending order. The ratio

$$100\left(\frac{\sum_{i=1}^M \lambda_i}{\sum_{i=1}^N \lambda_i}\right) \tag{3}$$

is used to determine the number of POD basis functions to construct. The quantity in (3) provides a measure of the ensemble energy that is captured by a POD basis consisting of M modes. By requiring a percentage of the energy contained in the snapshot ensemble be contained in the basis, the smallest value of M is calculated such that the quantity in (3) is greater than or equal to that percentage.

The eigenvectors $\{v_i\}_{i=1}^M$ corresponding to the M eigenvalues of largest magnitude are calculated. Each eigenvector is normalized so that

$$\|v_i\|^2 = \frac{1}{\lambda_i}. \tag{4}$$

The orthonormal POD basis set $\{\phi_i(\mathbf{x})\}_{i=1}^M$ is constructed according to

$$\phi_i(\mathbf{x}) = \sum_{j=1}^N v_{i,j} S_j(\mathbf{x}), \tag{5}$$

where $v_{i,j}$ is the j^{th} component of v_i. With the basis in hand, the system solution $w(t,\mathbf{x})$ is approximated as a linear combination of POD modes, i.e.,

$$w(t,\mathbf{x}) \approx \sum_{i=1}^M \alpha_i(t)\phi_i(\mathbf{x}). \tag{6}$$

Split-POD

Using an energy argument based on (3) is a convenient way to determine the number of POD modes needed for the reduced model. However, blindly applying (3) to determine the necessary number of modes is problematic in a boundary control setting. In boundary control applications, it is desired that control input energy be as small as possible while still satisfying the control objective. For example, in flow control applications where the control is located on a surface, it is desired that small control inputs yield large changes in the flow field behavior.[23] In essence, effects of small control inputs are amplified by the natural instabilities and comparatively high energy content of the baseline flow field. Simply applying (3) to an ensemble consisting of baseline and actuated data presents the risk of important structures due to control input being discarded. These structures are typically of much lower energy content than those associated with the baseline solution. For these reasons, we extend the POD algorithm described above so that baseline and control input energy are considered separately. We refer to this method as split-POD. The basis resulting from this method will consist of modes significant to the baseline solution as well as those significant from an actuation standpoint.

The basic idea is to decompose each snapshot in the ensemble into a component in the span of a baseline POD basis and an orthogonal component. This is done by employing useful properties of orthogonal projections on Hilbert spaces.[24] By considering the case of baseline and actuated data separately, the orthogonal component is constructed such that it contains new information due to the control input.

An ensemble of solution snapshots is generated for the case of zero control input. From this baseline snapshot ensemble, a set of POD modes is constructed that contains a high percentage of the baseline energy. For notational convenience, denote this baseline basis by $\{\xi_j\}_{j=1}^{\bar{M}_B}$ where $\bar{M}_B$ is the number of modes. By employing the energy ratio in (3), we choose $\bar{M}_B$ so that the baseline basis contains most of the energy contained in the baseline snapshot ensemble.

With a large set of baseline modes in hand, an ensemble of solution snapshots is generated for the case of nonzero control input. Denote the actuated ensemble by $\{T_i\}_{i=1}^{N_A}$ where N_A is the number of actuated snapshots.

For each snapshot in the actuated ensemble, we determine the component that is in the span of the baseline basis. In particular, define b_{ij} according to

$$b_{ij} = \langle T_i, \xi_j \rangle, 1 \le i \le N_A, 1 \le j \le \bar{M}_B. \tag{7}$$

Then, b_{ij} is the projection of the ith actuated snapshot T_i onto the jth baseline POD mode ξ_j. In other words, the product $b_{ij}\xi_j$ is the component of T_i that is in the direction of ξ_j. The linear combination $\sum_{j=1}^{\bar{M}_B} b_{ij}\xi_j$ is the component of T_i in the span of the baseline basis.

Define $\bar{T}_i$ according to

$$\bar{T}_i = T_i - \sum_{j=1}^{\bar{M}_B} b_{ij}\xi_j. \tag{8}$$

Then, $\bar{T}_i$ is the component of T_i not contained in the span of the high order baseline basis. As T_i is a solution snapshot for the case of nonzero control input, $\bar{T}_i$ consists of new information due to the control input. A second set of POD modes is constructed from the data ensemble $\{\bar{T}_i\}_{i=1}^{N_A}$. Denote this set of "actuator modes" by $\{\eta_i\}_{i=1}^{M_A}$, where M_A is the number of modes. The energy ratio in (3) is used to determine M_A such that the basis of actuator modes contains an arbitrary amount of the additional energy resulting from the control input. We have employed the high order baseline basis to extricate new information resulting from the control. Having done that, the baseline basis is now truncated to contain a more reasonable number of modes for model development. Denote M_B as the number of baseline modes retained after truncation with corresponding basis set $\{\xi_j\}_{j=1}^{M_B}$

To simplify reduced order modeling via Galerkin projection, it is advantageous to use a basis consisting of orthonormal modes. We now show that the sets of baseline and actuator modes can be combined into an overall basis set where all modes are orthonormal.

By construction, baseline modes are orthonormal. Similarly, actuator modes are orthonormal. Consider the inner product of ξ_k and $\bar{T}_i$ for arbitrary i, k. We see that

$$\left\langle \bar{T}_i, \xi_k \right\rangle = \left\langle T_i - \sum_{j=1}^{\bar{M}_B} b_{ij}\xi_j, \xi_k \right\rangle \tag{9}$$

$$= \langle T_i, \xi_k \rangle - \sum_{j=1}^{\bar{M}_B} b_{ij} \langle \xi_j, \xi_k \rangle . \tag{10}$$

As the baseline modes are orthonormal, $\langle \xi_j, \xi_k \rangle = 0$ unless $j = k$. For $j = k$, $\langle \xi_j, \xi_k \rangle = 1$. As a result,

$$\langle T_i, \xi_k \rangle - \sum_{j=1}^{\bar{M}_B} b_{ij} \langle \xi_j, \xi_k \rangle = \langle T_i, \xi_k \rangle - b_{ik}. \tag{11}$$

By definition (7), $b_{ik} = \langle T_i, \xi_k \rangle$. Thus, we have

$$\left\langle \bar{T}_i, \xi_k \right\rangle = 0, \text{ for arbitrary } i, k. \tag{12}$$

From (5), each actuator mode η_i is a linear combination of the snapshots $\{\bar{T}_i\}_{i=1}^{N_A}$. As a result, (12) in combination with the linearity of the inner product yields

$$\langle \eta_i, \xi_k \rangle = 0, \text{ for arbitrary } i, k. \tag{13}$$

Therefore, we have

$$\{\eta_i\} \perp \{\xi_j\}. \tag{14}$$

This result allows us to combine the baseline and actuator modes into an overall basis set

$$\{\phi_i\}_{i=1}^{M_B+M_A} = \{\xi_1, \xi_2, ..., \xi_{M_B}, \eta_1, \eta_2, ..., \eta_{M_A}\}, \tag{15}$$

where all modes in the basis are orthonormal. The system solution $w(t, \mathbf{x})$ is still approximated as a linear combination of modes as in (6). Moreover, separate consideration of baseline and actuated energy allows us to write this linear combination as

$$w(t, \mathbf{x}) \approx \sum_{j=1}^{M_B} \theta_j(t)\xi_j(\mathbf{x}) + \sum_{i=1}^{M_A} \beta_i(t)\eta_i(\mathbf{x}), \tag{16}$$

where $\{\theta_j\}_{j=1}^{M_B}$ and $\{\beta_i\}_{i=1}^{M_A}$ are temporal coefficients for the baseline and actuator basis, respectively. This allows us to consider the system solution as a baseline component and an additional component induced by the control input.

Model Problem

We now demonstrate the benefit of careful consideration of actuated dynamics on reduced model accuracy and subsequent boundary control effectiveness. A distributed parameter system is formulated which models convective flow over an obstacle. Let $\Omega_1 \subseteq \mathbb{R}^2$ be the rectangle given by $(a, b] \times (c, d)$. Let $\Omega_2 \subseteq \Omega_1$ be the rectangle given by $[a_1, a_2] \times [b_1, b_2]$ where $a < a_1 < a_2 < b$ and $c < b_1 < b_2 < d$. The problem domain, Ω, is given by $\Omega = \Omega_1 \setminus \Omega_2$. In this configuration, Ω_2 is the obstacle. Dirichlet boundary controls are located on the obstacle bottom and top, denoted by Γ_B and Γ_T, respectively.

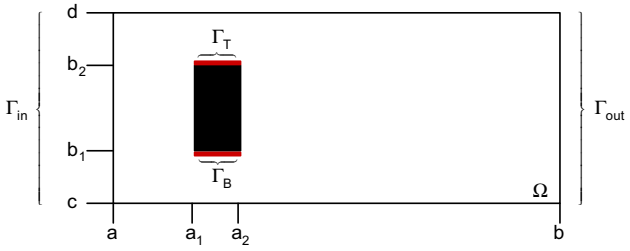

Figure 1: Problem Geometry.

The dynamics of the system are described by the two-dimensional Burgers equation

$$\frac{\partial}{\partial t} w(t, x, y) + \nabla \cdot F(w) = \frac{1}{Re} \Delta w(t, x, y) \tag{17}$$

for $t > 0$ and $(x, y) \in \Omega$. In (17), $F(w)$ has the form

$$F(w) = \left[C_1 \frac{w^2(t, x, y)}{2} \qquad C_2 \frac{w^2(t, x, y)}{2} \right]^T, \tag{18}$$

where C_1, C_2 are nonnegative constants. This equation has a convective nonlinearity like that found in the Navier-Stokes momentum equation modeling fluid flow.[25] The quantity Re, a nonnegative constant, is analogous to the Reynolds number in the Navier-Stokes momentum equation.

To complete the model of the system, boundary conditions must be specified as well as an initial condition. For simplicity, boundary controls are assumed to be separable. With this assumption, we specify conditions on the obstacle bottom and top of the form

$$w(t, \Gamma_B) = u_B(t) \Psi_B(x), \tag{19}$$

$$w(t, \Gamma_T) = u_T(t) \Psi_T(x). \tag{20}$$

In (19)-(20), $u_B(t)$ and $u_T(t)$ are the controls on the bottom and top of the obstacle, respectively. The profile functions $\Psi_B(x)$ and $\Psi_T(x)$ describe the spatial influence of the controls on the boundary. A parabolic inflow condition is specified of the form

$$w(t, \Gamma_{in}) = f(y). \tag{21}$$

At the outflow, a Neumann condition is specified according to

$$\frac{\partial}{\partial x} w(t, \Gamma_{out}) = 0. \tag{22}$$

For notational convenience, denote the remaining boundary as Γ_U. We require that values be fixed at zero along Γ_U as time evolves. The resulting boundary condition is of the form

$$w(t, \Gamma_U) = 0. \tag{23}$$

The initial condition of the system is given by

$$w(0, x, y) = w_0(x, y) \in L^2(\Omega). \tag{24}$$

As developed in previous work,[17] the reduced order state-space model for this system with explicit boundary control input is of the form

$$\dot{\alpha} = A\alpha + Bu + G(\alpha) + F. \tag{25}$$

Projecting the initial condition $w_0(x, y)$ onto the POD basis results in an initial condition for the reduced order model of the form

$$\alpha(0) = \alpha_0. \tag{26}$$

Open-Loop Comparisons

We demonstrate the impact of basis construction technique on the ability of the reduced model to represent dynamics induced by a boundary control input. Instantaneous snapshots are generated for (17), (19)-(24) via numerical simulation. A positive parabolic profile with unit maximum amplitude is specified for the inlet condition in boundary condition (21). In (18), we set $C_1 = 1$ and $C_2 = 0$ in order to obtain solutions that convect from left to right for the positive inlet. In addition, we specify that $Re = 300$. The problem domain Ω is discretized, resulting in a uniform grid with spatial step-size h. We utilize a finite difference scheme[26] to numerically solve the model problem with and without boundary control input. The resulting discretized system describes roughly 2,000 states.

We construct reduced order models from snapshot ensembles obtained for two scenarios. In the first scenario, snapshots are generated for the baseline solution and for boundary actuation at a fixed frequency. For the second case, snapshots are generated for the baseline solution and a more complicated chirp input where the frequency varies with time. For both scenarios, we compare model agreement resulting from combining baseline and actuated snapshots into an overall lumped snapshot ensemble to that obtained by decomposing snapshots into their baseline and actuated components and constructing the split-POD basis as in (15). In the results that follow, basis construction from a lumped snapshot ensemble is referred to as the "lumped" method. Constructing the basis by considering baseline and actuated energy separately is referred to as the "split" method.

Scenario 1

Snapshots are generated for the baseline solution and for the solution arising under periodic boundary actuation. Inputs specified are of the form

$$u_B(t) = sin(\pi t) \qquad u_T(t) = 0, \tag{27}$$

$$u_B(t) = 0 \qquad u_T(t) = sin(\pi t). \tag{28}$$

In (27), periodic actuation is done on the bottom of the obstacle while values along the obstacle top are held at zero. In (28), values along the obstacle bottom are held at zero with periodic actuation occurring at the top. For each control input listed in (27)-(28), snapshots are taken in increments of $\Delta t = 0.1$ starting from $t = 0$ and ending at $t = 15$. The steady baseline solution is used for the initial condition.

With an ensemble of snapshots in hand, ratio (3) is used to determine the number of basis modes to construct. Requiring that 99.9% of the ensemble energy be contained in the POD basis results in a lumped basis consisting of 7 modes. Separate consideration of baseline and actuated energy results in a split basis consisting of 1 baseline mode and 16 actuator modes.

We now employ linear combination (6) to compare boundary condition agreement between the full order system and reduced models obtained via the lumped and split-POD bases. By specifying characteristic functions for the control profiles $\Psi_B(x)$ and $\Psi_T(x)$ in (19)-(20), we see that

$$\sum_{i=1}^{M} \alpha_i(t)\phi_i(\Gamma_B) \approx w(t, \Gamma_B) = u_B(t), \tag{29}$$

$$\sum_{i=1}^{M} \alpha_i(t)\phi_i(\Gamma_T) \approx w(t, \Gamma_T) = u_T(t), \tag{30}$$

We construct the linear combinations on the left in (29)-(30) and compare them to the exact boundary conditions $u_B(t)$ and $u_T(t)$ specified in the full order system. We first perform comparisons for boundary inputs explicitly used during ensemble generation. Results obtained for the baseline solution and for the solution with periodic boundary actuation of the form $sin(\pi t)$ are shown in Figure 2. In that figure, dashed

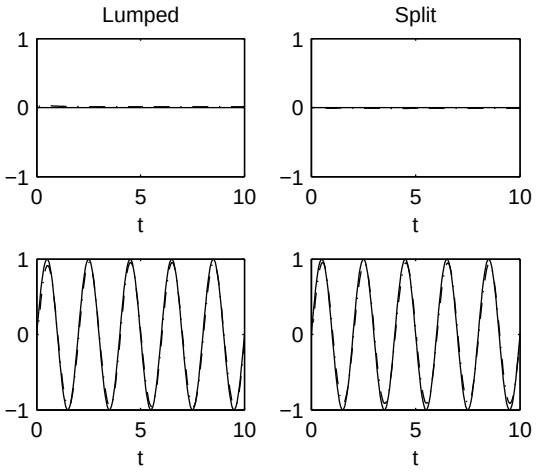

Figure 2: Boundary Condition Accuracy.

curves denote the linear combination of POD modes restricted to the boundary. Solid curves denote the exact full order boundary input. Results obtained for the lumped basis method are plotted on the left. Split-POD basis results are plotted on the right. As seen in Figure 2, both methods result in very good agreement between the exact boundary conditions and the linear combination of POD modes restricted to the boundary. Dashed and solid curves are virtually identical.

In a feedback control setting, dynamics induced by the control are typically not known a priori. The specifics of the control law and the dynamics induced by it are not known prior to ensemble creation. Typically, in the closed-loop system, the boundary input resulting from the control law will be different than the inputs used to generate the snapshot ensemble. As a result, it is useful to compare reduced and full order model agreement for inputs not specified during ensemble creation. This provides insight into the suitability of the reduced model for closed-loop control law design. For these reasons, we now compare boundary condition agreement between the reduced and full order systems for open-loop inputs that were not used during ensemble creation. Boundary inputs specified are of the form

$$u_B(t) = min\left(\frac{t}{3}, 1\right), \tag{31}$$

$$u_T(t) = sin\left(\frac{3}{2}\pi t\right). \tag{32}$$

Results obtained for the lumped and split basis methods are shown in Figure 3.

As seen in Figure 3, very good agreement is seen between the reduced and full order systems for the split method, even though the inputs considered were not specifically included in the snapshot ensemble. Condition (32) is reconstructed well using the lumped method. However, the reconstruction of the piecewise linear input in (31) is much less accurate when the lumped basis is used.

To further compare the lumped and split basis methods and their utility for control law design, we project the full order solution at each time step onto the lumped and split POD bases. The resulting temporal coefficients are compared to those predicted by the reduced order models. Boundary inputs specified are as in (31)-(32). Results obtained for the first 5 temporal coefficients of the lumped method are shown in Figure 4. The first 5 temporal coefficients for the split method are shown in Figure 5. In Figures 4-5, solid curves denote values of temporal coefficients obtained via the projection. Dashed curves denote the solution of the reduced order model. Overall, the accuracy of the split method is better, particularly for temporal coefficients with higher frequency content. Separate consideration of actuated energy during basis

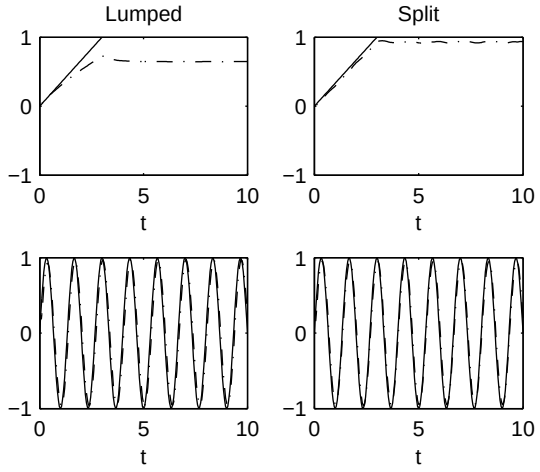

Figure 3: Boundary Condition Accuracy.

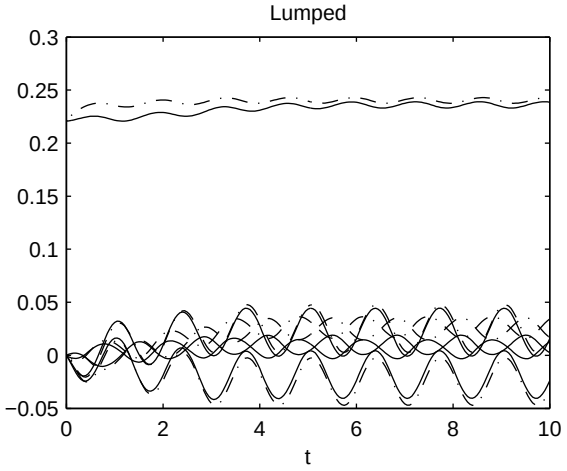

Figure 4: Temporal Coefficient Accuracy for the Lumped Method.

construction results in better representation of dynamics induced by boundary inputs not specified during ensemble creation. This is advantageous in a boundary feedback control setting where dynamics induced by the control are typically not known beforehand.

Scenario 2

It is likely that a snapshot ensemble for inputs at a single frequency results in a POD basis that does not adequately span the dynamics induced by a feedback control. Feedback controls designed from such a basis are bound to be ineffective when implemented in the full order system. In Scenario 2, we compare the lumped and split basis methods using a snapshot ensemble generated from chirp inputs of the form

$$u_B(t) = sin\left(\pi\left(e^t\right)^{0.3}\right) \qquad u_T(t) = 0, \tag{33}$$

$$u_B(t) = 0 \qquad u_T(t) = sin\left(\pi\left(e^t\right)^{0.3}\right). \tag{34}$$

As seen in Figure 6, an input of this form generates the system response over a range of frequencies. The resulting POD basis is much more likely to sufficiently span the unknown dynamics generated by a feedback control.

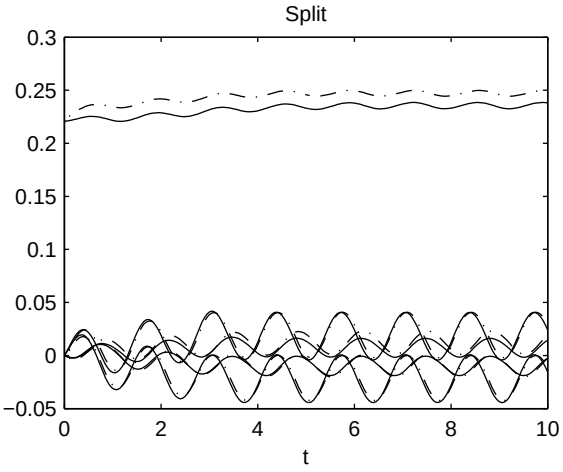

Figure 5: Temporal Coefficient Accuracy for the Split Method.

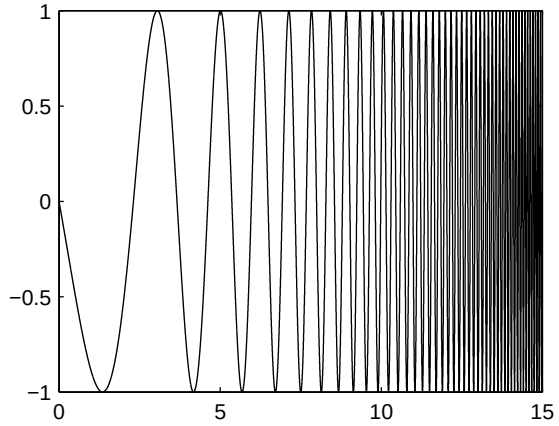

Figure 6: The input function $u = sin\left(\pi\left(e^t\right)^{0.3}\right)$.

Instantaneous snapshots are generated for the baseline solution as well as for solutions arising from the inputs in (33)-(34). For each control input listed in (33)-(34), snapshots are taken in increments of $\Delta t = 0.1$ starting from $t = 0$ and ending at $t = 15$. The steady baseline solution is used for the initial condition.

Requiring that 99.9% of the ensemble energy be contained in the POD basis results in a lumped basis consisting of 7 modes. A split basis comprised of 1 baseline mode and 25 actuator modes are needed when baseline and actuated energy is considered separately.

As in Scenario 1, we compare boundary condition accuracy of the lumped and split methods for boundary inputs not specified during ensemble generation. For the sake of comparison, we use the boundary conditions given by (31)-(32). Results obtained for the lumped and split basis methods are shown in Figure 7. As seen in that figure, very good boundary condition agreement is seen between the reduced and full order systems for both basis methods. In particular, by comparing Figures 3 and 7, we see that the piecewise linear boundary condition in (31) is represented much better by the lumped method when inputs (33)-(34) are used to generate the snapshot ensemble.

As before, we now project the full order solution at each time step onto the lumped and split POD bases. The resulting temporal coefficients are compared to those predicted by the reduced order models. The results for the lumped method are shown in Figure 8. Split method results are shown in Figure 9. As seen in those figures, the accuracy of the split method is better. For temporal coefficients with significant frequency content, values predicted by the reduced model are virtually identical to those obtained by projecting the full

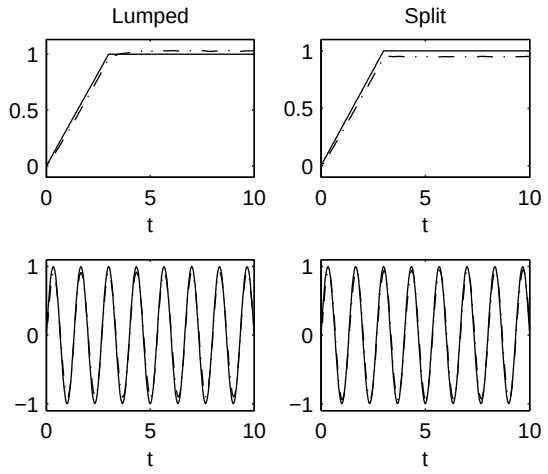

Figure 7: Boundary Condition Accuracy.

solution onto the split basis, even though the boundary inputs specified are different than those used during ensemble creation. The split method is better suited with regard to feedback control law design as it is more capable of accurately representing dynamics that are not explicitly included in the snapshot ensemble.

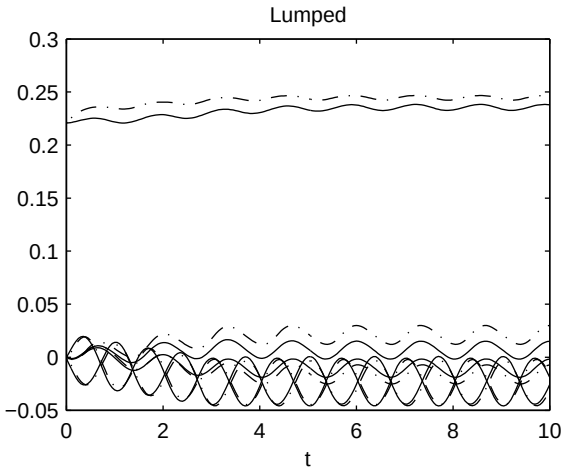

Figure 8: Temporal Coefficient Accuracy for the Lumped Method.

Closed-Loop Results

We now compare the effectiveness of the lumped and split-POD basis methods in a feedback control setting. The reduced system given by (25), (26) is linearized, yielding a state-space equation of the form

$$\dot{\alpha}(t) = A\alpha + Bu, \tag{35}$$

$$\alpha(0) = \alpha_0. \tag{36}$$

We consider the tracking problem for (35)-(36). A fixed reference signal $w_{ref}(\mathbf{x})$ is specified for the full order system. Projecting $w_{ref}(\mathbf{x})$ onto the POD basis yields tracking coefficients for the reduced order model, denoted by α_{ref}.

To formulate the tracking control problem, we consider the γ-shifted linear quadratic regulator (LQR) cost function

$$J(\alpha_0, u) = \int_0^\infty \left\{(\alpha - \alpha_{ref})^T Q(\alpha - \alpha_{ref}) + u^T R u\right\} e^{2\gamma t} dt. \tag{37}$$

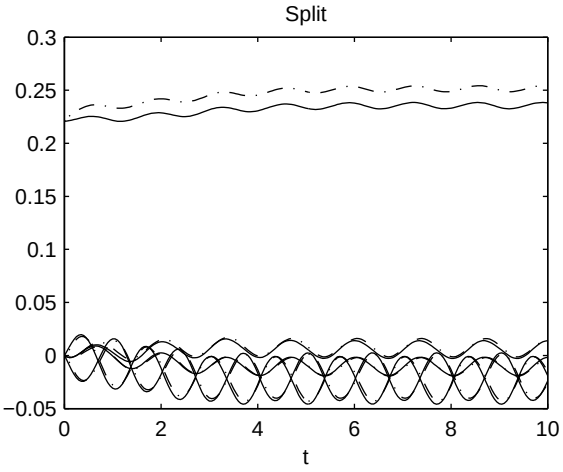

Figure 9: Temporal Coefficient Accuracy for the Split Method.

In (37), Q is a diagonal, symmetric, positive semi-definite matrix of state weights. R is a diagonal, symmetric, positive definite matrix of control weights. The quantity γ, a nonnegative constant, is an additional parameter that provides added robustness in the control.[27,28]

We use the LQR formulation in (37) to compare closed-loop results obtained from the lumped and split-POD basis methods. A snapshot ensemble is constructed containing baseline solution data as well as data

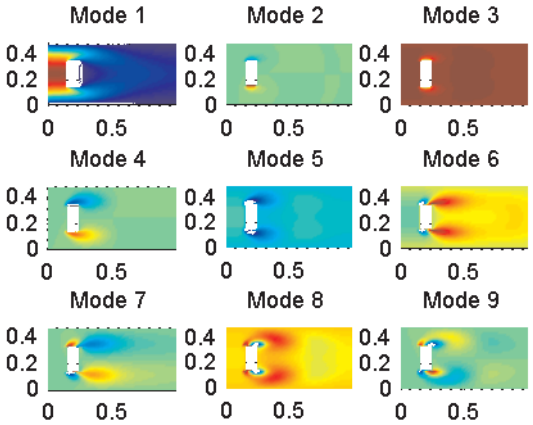

Figure 10: Split Basis Modes.

resulting from nonzero boundary actuation. As it is desired that the POD basis spans unknown dynamics introduced by the LQR feedback control, boundary inputs specified during ensemble creation are of the form

$$u_B(t) = Csin\left(\pi\left(e^t\right)^{0.3}\right) \qquad u_T(t) = 0, \tag{38}$$

$$u_B(t) = 0 \qquad u_T(t) = Csin\left(\pi\left(e^t\right)^{0.3}\right) \tag{39}$$

for $C = 1, 2, 3$.

For each control input listed in (38)-(39), snapshots are taken in increments of $\Delta t = 0.1$ starting from $t = 0$ and ending at $t = 15$. The steady baseline solution is specified for the initial condition. The resulting snapshot ensemble consists of roughly 900 snapshots. Requiring that 99% of the ensemble energy be contained in the POD basis results in a lumped basis consisting of 5 modes. A split basis comprised of 1 baseline mode

and 20 actuator modes is needed when baseline and actuated energy are considered separately. The first 9 modes of the split basis are shown in Figure 10. In that figure, mode 1 is the baseline mode. Modes 2-9 are actuator modes.

The tracking LQR problem requires the specification of the reference signal α_{ref}. In the results that follow, α_{ref} is obtained from the unactuated steady solution for the case $Re = 50$. This solution is projected

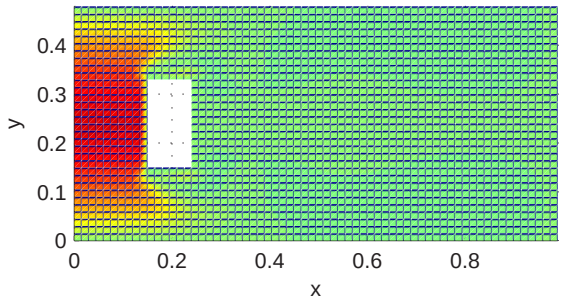

Figure 11: Tracking Reference Function.

onto the lumped and split bases. The temporal values obtained are used as tracking coefficients in the reduced order control problem. The reference signal obtained by projecting the steady solution at $Re = 50$ onto the split basis is shown in Figure 11. The reference function obtained by projecting onto the lumped basis is similar. To complete the control formulation, each state in the reduced order model is prescribed a weight of 2,500. The two boundary controls are each given unit weight. The value specified for γ in (37) is 0.25. The closed-loop solution of the reduced order model constructed with the split POD basis is shown in Figure 12. By comparing the controlled solution of Figure 12 to the reference function in Figure 11, it is apparent

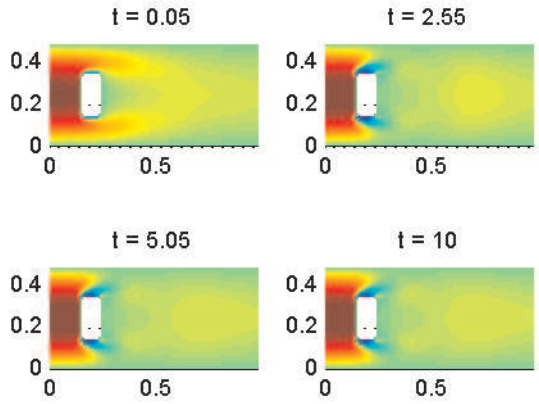

Figure 12: Closed-Loop Split Model.

that the closed-loop reduced order model satisfies the control objective quite well. Separate consideration of actuated energy in the split POD basis method results in satisfactory tracking of the reference signal.

When the energy ratio in (3) is applied to baseline and actuated data lumped together into an overall snapshot ensemble, the results are much less favorable. Closed-loop solutions of the reduced order model constructed with the lumped POD basis are shown in Figure 13. As seen in that figure, virtually no tracking is achieved by the reduced order control. Adjusting parameters in the control formulation has little effect on this result. Increasing the state-weights and the parameter γ to 10,000 and 0.75, respectively, does not significantly improve the performance of the control. System information relevant from a control standpoint

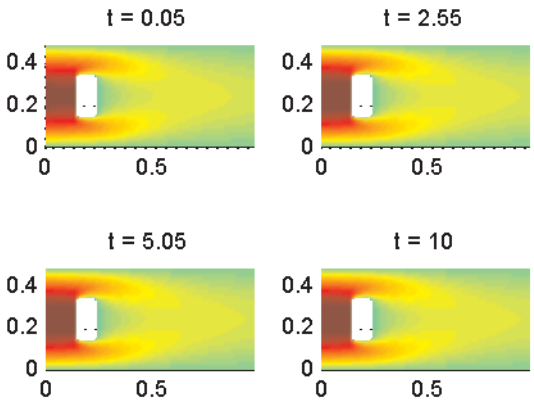

Figure 13: Closed-Loop Lumped Model.

is discarded when an energy argument is applied during order reduction to the lumped snapshot ensemble containing baseline and actuated data. The resulting reduced order model does not adequately describe dynamics induced by the control. Consequently designing a feedback control from such a model results in very ineffective response when the control is applied to the system.

Full Order Validation

To validate the effectiveness of the reduced order control obtained via the split basis method, we utilize a fixed-point projection algorithm[16] to incorporate the reduced order boundary control in the full order model. The closed-loop solution of the full order system is shown in Figure 14. As seen in that figure, the reduced

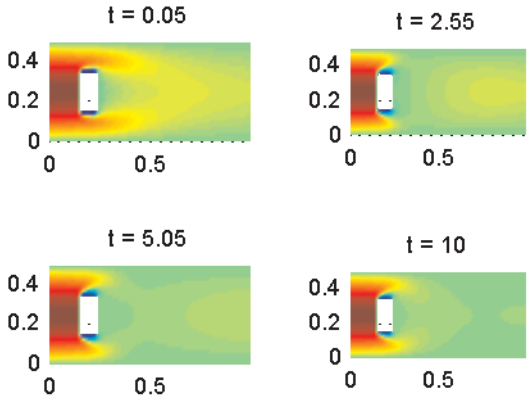

Figure 14: Closed-Loop Response with Split Method Feedback Control.

order control effectively drives the full order plant to the target profile. The full order discretized model is comprised of roughly 2,000 states. The reduced model obtained via the split basis method describes 21 states. As a result, system dimension is reduced by roughly two orders of magnitude with the resulting reduced order control being quite effective.

Conclusions

In this paper, a reduced basis construction method was developed allowing for separate consideration of baseline and actuated dynamics in the reduced modeling process. A prototype initial boundary value

problem, governed by the two-dimensional Burgers equation, was formulated to demonstrate the utility of the method. When actuated energy was considered separately, much better agreement was seen between open-loop solutions of the reduced and full order systems. Separate consideration of energy induced by the boundary control resulted in effective feedback control for the reduced and full order systems. When actuated energy was not explicitly accounted for in the reduced modeling process, the resulting feedback control was completely ineffective when applied to the system.

These results demonstrate the need for separate consideration of baseline and actuated energy in the reduced modeling process when the resulting model is to be used for feedback control law design. Basis construction relying on an energy argument applied to a lumped snapshot ensemble containing baseline and actuated data can result in important control information being discarded during order reduction. This is particularly the case in a boundary control setting where ensemble energy is typically dominated by that in the baseline data. Feedback controls developed from the resulting reduced model are likely ineffective when applied to the system. Separate consideration of dynamics induced by boundary control input results in reduced order controllers that are much more effective when applied to the reduced and full order systems.

In a companion paper,[20] we apply these methods in an experimental laser turret application with the control objective of regularizing the unsteady flow over the turret.

References

[1] Anderson, J., *Computational Fluid Dynamics*, McGraw-Hill, New York, 1995, pp. 3-31.

[2] Kirk, D., *Optimal Control Theory*, Dover Publications, New York, 2004, pp. 90-93.

[3] Antoulas, A., *Approximation of Large-Scale Dynamical Systems*, Society for Industrial and Applied Mathematics, Philadelphia, 2005, pp. 2-24.

[4] Atwell, J. and King, B., "Computational Aspects of Reduced Order Feedback Controllers for Spatially Distributed Systems," *Proceedings of the 38th IEEE Conference on Control and Desicion*, December 1999, pp. 4301-4306.

[5] Ausseur, J., Pinier, J., Glauser, M., and Higuchi, H., "Experimental Development of a Reduced Order Model for Flow Separation Control ," AIAA Paper 2006-1251, January 2006.

[6] Ausseur, J., Pinier, J., and, Glauser, M., "Flow Separation Control Using a Convection Based POD Approach ," AIAA Paper 2006-3017, June 2006.

[7] Banks, H., del Rosario, R., and Smith, R., "Reduced Order Model Feedback Control Design: Numerical Implentation in a Thin Shell Model," Technical Report CRSC-TR98-27, Center for Research in Scientific Computation, North Carolina State University, June, 1998.

[8] Caraballo, E., Samimy, M., and DeBonis, J., "Low Dimensional Modeling of Flow for Closed-Loop Flow Control," AIAA Paper 2003-0059, January 2003.

[9] Caraballo, E., Yuan, X., Little, J., Debaisi, M., Serrani, A., Myatt, J., and Samimy, M., "Further Development of Feedback Control of Cavity Flow Using Experimental Based Reduced Order Model ," AIAA Paper 2006-1405, January 2006.

[10] Cohen, K., Siegel, S., McLaughlin, T., and Myatt, J., "Proper Orthogonal Decomposition Modeling of a Controlled Ginzburg-Landau Cylinder Wake Model," AIAA Paper 2003-2405, January 2003.

[11] Cohen, K., Siegel, S., Seidel, J., and, McLaughlin, T., "Reduced Order Modeling for Closed-Loop Control of Three Dimensional Wakes," AIAA Paper 2006-3356, June 2006.

[12] Efe, M. and Ozbay, H., "Proper Orthogonal Decomposition for Reduced Order Modeling: 2D Heat Flow," *Proc. of 2003 IEEE Conference on Control Applications*, June 23-25, 2003, pp. 1273-1277.

[13] Luchtenburg, M., Tadmore, G., Lehmann, O., Noack, B., King, R., and Morzynski, M., "Tuned POD Galerkin Models for Transient Feedback Regulation of the Cylinder Wake," AIAA Paper 2006-1407, January 2006.

[14] Siegel, S., Cohen, K., Seidel, J., and McLaughlin, T., "Proper Orthogonal Decomposition Snapshot Selection for State Estimation of Feedback Controlled Flows ," AIAA Paper 2006-1400, January 2006.

[15] Kasnakoğlu, C., Serrani, A., and Efe, M., "Control Input Separation by Actuation Mode Expansion for Flow Control Problems," *International Journal of Control* (in review).

[16] Camphouse, R.C., "Boundary Feedback Control Using Proper Orthogonal Decomposition Models," *Journal of Guidance, Control, and Dynamics*, Vol. 28, No. 5, September-October 2005, pp 931-938.

[17] Camphouse, R. C. and Myatt, J. H., "Reduced Order Modelling and Boundary Feedback Control of Nonlinear Convection," AIAA Paper 2005-5844, August 2005.

[18] Carlson, H., Glauser, M., Higuchi, H., and Young, M., "POD Based Experimental Flow Control on a NACA-4412 Airfoil," AIAA Paper 2004-0575, January 2004.

[19] Carlson, H., Glauser, M., and Roveda, R., "Models for Controlling Airfoil Lift and Drag," AIAA Paper 2004-0579, January 2004.

[20] Wallace, R. D., Andino, M. Y., Glauser, M. N., Schmit, R. F., Camphouse, R. C., and Myatt, J. H., "Flow and Aero-Optics Around a Turret Part 2: Surface Pressure Based Proportional Closed-Loop Flow Control," AIAA Paper 2008-4217, June 2008.

[21] Holmes, P., Lumley, J., and Berkooz, G., *Turbulence, Coherent Structures, Dynamical Systems and Symmetry*, Cambridge University Press, New York, 1996, pp. 86-127.

[22] Sirovich, L., "Turbulence and the Dynamics of Coherent Structures, Parts I-III," *Quarterly of Applied Mathematics*, Volume 45, Brown University, Rhode Island, 1987, pp. 561-590.

[23] Gad el Hak, M., *Flow Control: Passive, Active, and Reactive Flow Management*, Cambridge University Press, New York, 2000, pp. 318-357.

[24] Debnath, L. and Mikusiński, P., *Introduction to Hilbert Spaces with Applications*, Academic Press, California, 1999, pp. 87-130.

[25] Batchelor, G., *An Introduction to Fluid Dynamics*, Cambridge University Press, New York, 1999, pp. 147.

[26] Camphouse, R. and Myatt, J., "Feedback Control for a Two-Dimensional Burgers Equation System Model," AIAA Paper 2004-2411, June 2004.

[27] Burns, J. and Kang, S., "A Control Problem for Burgers Equation with Bounded Input/Output," *Nonlinear Dynamics*, Volume 2, Kluwer Academic Publishing, New York, 1991, pp. 235-262.

[28] Burns, J. and Kang, S., "A Stabilization Problem for Burgers Equation with Unbounded Control and Observation," *Control and Estimation of Distributed Parameter Systems*, Volume 100, Birkhauser Verlag, Basel, 1991, pp. 51-72.